RL-TR-94-137
Final Technical Report
August 1994

DEVELOPMENT OF ULTRASHORT OPTICAL PULSE SOURCES NEAR 1.3 AND 1.5 MICRONS WITH AN EMPHASIS ON STABILITY, HIGH REPETITION RATE, AND PARALLELISM

Rensselaer Polytechnic Institute

R.L. Fork

APPROVED FOR PUBLIC RELEASE; DISTRIBUTION UNLIMITED.

Rome Laboratory
Air Force Materiel Command
Griffiss Air Force Base, New York

This report has been reviewed by the Rome Laboratory Public Affairs Office (PA) and is releasable to the National Technical Information Service (NTIS). At NTIS it will be releasable to the general public, including foreign nations.

RL-TR-94-137 has been reviewed and is approved for publication.

APPROVED:

STEVEN T. JOHNS
Project Engineer

FOR THE COMMANDER:

LUKE L. LUCAS, Colonel, USAF
Deputy Director of Surveillance & Photonics

If your address has changed or if you wish to be removed from the Rome Laboratory mailing list, or if the addressee is no longer employed by your organization, please notify RL (OCPA) Griffiss AFB NY 13441. This will assist us in maintaining a current mailing list.

Do not return copies of this report unless contractual obligations or notices on a specific document require that it be returned.

REPORT DOCUMENTATION PAGE

Form Approved
OMB No. 0704-0188

1. AGENCY USE ONLY (Leave Blank)	2. REPORT DATE	3. REPORT TYPE AND DATES COVERED
	August 1994	Final May 93 - May 94

4. TITLE AND SUBTITLE
DEVELOPMENT OF ULTRASHORT OPTICAL PULSE SOURCES NEAR 1.3 AND 1.5 MICRONS WITH AN EMPHASIS ON STABILITY, HIGH REPETITION RATE, AND PARALLELISM

5. FUNDING NUMBERS
C - F30602-93-C-0104
PE - 62702F
PR - 4600
TA - P1
WU - PP

6. AUTHOR(S)
R.L. Fork

7. PERFORMING ORGANIZATION NAME(S) AND ADDRESS(ES)
Rensselaer Polytechnic Institute
110 Eighth Street
Troy NY 12180-3590

8. PERFORMING ORGANIZATION REPORT NUMBER
N/A

9. SPONSORING/MONITORING AGENCY NAME(S) AND ADDRESS(ES)
Rome Laboratory/OCPA
25 Electronic Pky
Griffiss AFB NY 13441-4515

10. SPONSORING/MONITORING AGENCY REPORT NUMBER
RL-TR-94-137

11. SUPPLEMENTARY NOTES
Rome Laboratory Project Engineer: Steven T. Johns/OCPA/(315) 330-4456

12a. DISTRIBUTION/AVAILABILITY STATEMENT
Approved for public release; distribution unlimited.

12b. DISTRIBUTION CODE

13. ABSTRACT (Maximum 200 words)
We use experiment and numerical simulation to study performance of a harmonically modelocked laser that includes an electronic modulator and an intracavity Fabry-Perot etalon. We experimentally generate trains of pulses of 40 ps duration at 1.3 GHz. We also study introduction of nonlinear optical shaping in the form of a NOLM loop. Numerical simulation indicates that the NOLM loop, or similar nonlinear optical pulse shaping, can reduce the pulse duration to subpicosecond values. Experiment shows that the added length of a NOLM loop, however, has a destabilizing influence in that it tends to allow excitation of more than one supermode. Means of producing alternative nonlinear shaping that is not susceptible to this destabilization are examined. Dynamics of this type of laser, including NOLM loops, are simulated in a manner that predicts the rate of approach to stability.

14. SUBJECT TERMS
Modelocked lasers, Fiber lasers, Solitons, Ultrafast optics

15. NUMBER OF PAGES
36

16. PRICE CODE

17. SECURITY CLASSIFICATION OF REPORT	18. SECURITY CLASSIFICATION OF THIS PAGE	19. SECURITY CLASSIFICATION OF ABSTRACT	20. LIMITATION OF ABSTRACT
UNCLASSIFIED	UNCLASSIFIED	UNCLASSIFIED	UNLIMITED

TABLE OF CONTENTS

ABSTRACT 1
1. INTRODUCTION 1
2. EXPERIMENTAL LASER 2
3. FREE SPACE COMPONENTS OF THE LASER 4
4. FIBER COMPONENTS 7
5. PUMP SOURCE AND DIAGNOSTIC EQUIPMENT 8
6. SPECTRAL CONSTRAINTS ON THE HARMONICALLY MODELOCKED LASER 9
7. PULSE REPETITION RATE ETALON 11
8. FEEDBACK SYSTEM 12
9. EXPERIMENTAL FIGURE EIGHT VERSIONS OF THE LASER 14
10. NUMERICAL SIMULATIONS OF THE HML LASER 15
11. NUMERICAL SIMULATION OF THE MODELOCKED FIBER LASER INCLUDING A NOLM LOOP 17
12. SYNCHRONIZATION OF HML LASERS THAT INCLUDE NONLINEAR GATES 22
13. SOLUTIONS 24
14. CONCLUSIONS 24
15. ACKNOWLEDGMENTS 24
16. REFERENCES 25

Final Report: Development of Ultrashort Optical Pulse Sources Near 1.3 and 1.5 Microns with an Emphasis on Stability, High Repetition Rate and Parallelism

ABSTRACT

We use experiment and numerical simulation to study performance of a harmonically modelocked laser that includes an electronic modulator and an intracavity Fabry-Perot etalon. We experimentally generate trains of pulses of 40 ps duration at 1.3 GHz. We also study introduction of nonlinear optical shaping in the form of a NOLM loop. Numerical simulation indicates that the NOLM loop, or similar nonlinear optical pulse shaping, can reduce the pulse duration to subpicosecond values. Experiment shows that the added length of a NOLM loop, however, has a destabilizing influence in that it tends to allow excitation of more than one supermode. Means of producing alternative nonlinear shaping that is not susceptible to this destabilization are examined. Dynamics of this type of laser, including NOLM loops, are simulated in a manner that predicts the rate of approach to stability

1. INTRODUCTION

Modelocked fiber lasers have generated stable trains of transform limited pulses at gigabit rates[1]. Other modelocked fiber lasers have generated pulses with durations of 1 picosecond or less.[2,3] There remains the task of obtaining stable trains of transform limited pulses with subpicosecond duration in a single user friendly system. In this paper we describe an experimental and calculational effort that explores this task. The basis of the effort is an experimental harmonically modelocked laser.

In general, it is important to provide stable near transform limited pulses for reliable communication systems. Chirped or asymmetric pulses shed energy in the form of dispersive wave radiation that becomes an additional source of noise that can increase the probability of errors. Modelocked semiconductor lasers, in particular, tend to produce asymmetric or chirped pulses that are undesirable. Optical fiber lasers, on the other hand, offer transform limited ultrashort optical pulses. They also offer high average power levels and strategies for effective pulse shortening. We consequently focus attention here solely on fiber lasers.

Harmonically modelocked fiber lasers, in particular, offer stable trains of transform limited ultrashort pulses at high repetition rates. A key problem is that there are a series of N

more or less independent "supermodes" where N is the ratio of the modulation frequency to the ring mode spacing. Each supermode consists of a group of coupled ring modes spaced apart by the modulation frequency. If two or more such supermodes lase simultaneously, the laser output suffers large amplitude swings at the beat frequency of the supermodes. Such fluctuations are unacceptable in a low error rate transmission source. We discuss the implications of these conditions and examine strategies for incorporating the desirable features in a single laser.

2. EXPERIMENTAL LASER

The selection of one supermode is achieved in the laser that we have built, Fig. 1, by using a technique developed by Harvey and Mollenauer[1]. A high finesse etalon having a free spectral range equal to the desired pulse repetition rate is introduced in the resonator. In this case, only the supermode whose frequencies match the peaks of this "pulse repletion rate etalon" can lase. An exception occurs when the modes drift due to changes in the ring length and two adjacent supermodes become symmetrically spaced around the peak of the etalon, with neither one dominant. The primary strategy for avoiding this condition is via active stabilization of the ring length. We discuss techniques for that stabilization below.

We also explored the task of introducing additional nonlinear optical pulse shortening mechanisms while retaining the desirable pulse stabilization and shaping features of the harmonically modelocked laser under construction. The goal is both very short pulses and also stable pulse trains and pulse envelopes. This aspect of the work departs from the earlier work of Harvey and Mollenauer in that it involves introducing additional structures within the laser for nonlinear pulse shortening. The principal structure we have explored is the nonlinear loop mirror (NOLM). We use both numerical simulation and experimental introduction of such loops in the laser. The numerical simulation work retains close contact with the experimental work by using parameters in the simulations from the experimental laser.

We divide the discussion of the laser structure and related apparatus into three categories; the free space components, the in line fiber components, and the diagnostic equipment. The use of both free space and fiber components is advantageous in this research stage in that the approach provides means for exploring the influence of a number of different kinds of components.

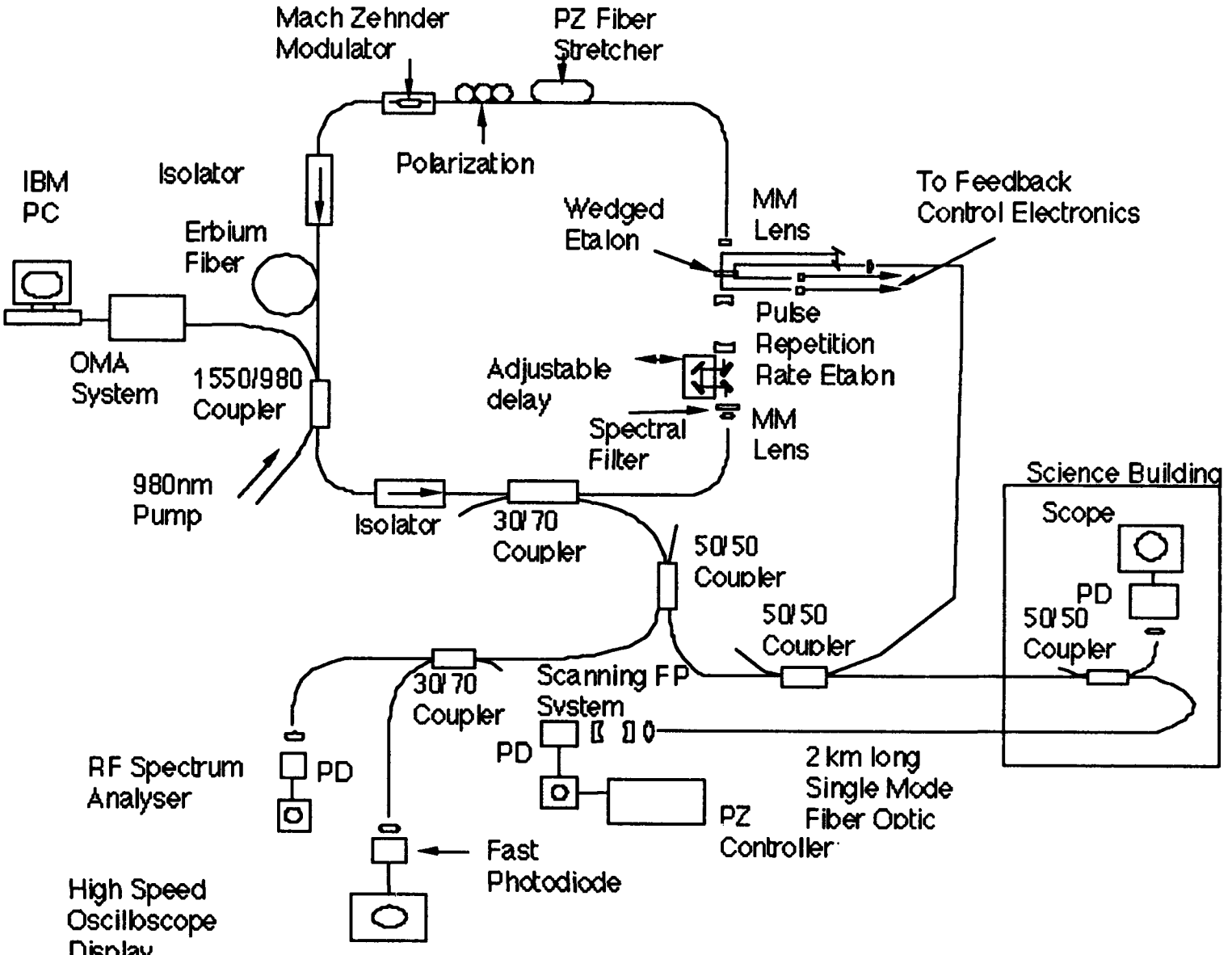

Fig. 1 Experimental apparatus

3. FREE SPACE COMPONENTS OF THE LASER

The free space components are important in that they provide adjustable means for controlling the laser operation. The components in free space are the collimating lenses, the positioners that hold the collimating lenses, the pulse repetition rate etalon, the wedged etalon, the free space delay line, and the spectral filter. Mode matching (MM) lenses are also included. The pulse repetition rate etalon achieves stability by using a super invar structure and spherical mirrors that are epoxied in position so that thermal drift and mechanical instabilities are minimized.

The fixed mirrors of the pulse repetition rate etalon provide increased stability, but also remove the usual opportunities for individual alignment and adjustment of the mirrors. We developed a means for epoxying the mirrors in position while monitoring the alignment during setting of the epoxy. The use of a slow setting epoxy and monitoring and readjustment during the setting up process is necessary to achieving mirrors sufficiently close to parallelism that final alignment can be achieved by orientation of the interferometer as a whole with respect to the beam.. Final alignment of the interferometer with the laser beam requires the use of monitor beams passed through the interferometer. The interferometer is scanned in length and the interferometer transmission spectrum examined so as to obtain an alignment condition such that the incident beam is mode matched into the lowest order transverse mode of the interferometer. The mirrors have 10 cm radii of curvature, a spacing of 11.0 cm and a FSR of 1.36 GHz.

The presence of the pulse repetition rate etalon in the laser stabilizes the pulse repetition rate, but it also places constraints on the other components of the laser. A basic constraint is that the round trip optical path through the laser must be an integral multiple of the spacing between the mirrors of the pulse repetition rate etalon. We include a free space delay line to facilitate adjustment of the total resonator path so as to satisfy this condition. The free space delay line must also be adjusted so as to maintain the laser beam in alignment with the fibers. This is demanding given the small aperture presented by the fiber and the need to have a free space region that is a significant fraction of a meter in length.

The free space delay line is located near the exit to the free space region. This avoids misalignment of the beam that is mode matched into the interferometer. We also provide means for readjusting the lens that couples the light back into the fiber at

the exit to the free space region via a differential screw driven xy positioner so that small corrections for the small redirections caused by translating the free space delay components can be made. Additional components in the free space section are the spectral filter and a wedged etalon. The spectral filter is located on a rotating post that allows the filter to be adjusted as to transmission wavelength. We locate the spectral filter after the pulse repetition rate etalon. This avoids a misalignment of the mode matching into the pulse repetition rate etalon caused by the varying offset of the beam introduced by rotating the filter. Small offsets of the beam into the fiber at the exit to the free space delay line can be corrected by small adjustments of the lens that couples the beam back into the fiber at the exit to the free space region.

The laser beam enters the free space region and is collimated by the lens that follows the fiber at this entrance. The lens is an 8 mm focal length laser diode collimating lens. The fiber end is cut at 8 degrees to minimize back reflections into the fiber path. The wedged etalon is located immediately after the collimating lens and has a low reflectance coating. The etalon is mounted on a translator that allows both x and y adjustments. The y adjustment allows the section of the etalon through which the laser beam passes to be varied in thickness by varying the position on the wedge where the laser beam intersects the wedge. This changes the central frequency of the laser oscillation by small amounts and allows a fine tuning of the laser frequency. The x adjustment allows an uncoated region of the etalon to be aligned with the laser beam for cases where minimum finesse of the wedged etalon is sought. This option is desirable since the wedged etalon introduces a spectral limitation that is more severe than the spectral filter and can become the limiting constraint on realization of shorter pulses. The bandwidth of the wedged etalon is about 60 GHz.

Means are also provided for introducing two monitoring beams for the feedback circuitry derived from the laser output. These beams pass above and below the region of the wedged etalon through which the laser beam passes. These beams provide an error signal used to maintain the pathlength of the laser at a fixed value.

The differential signal is obtained as follows: One beam passes through the wedged etalon at a point where the etalon is slightly thicker. The other beam through a region where the etalon is slightly thinner than the region where the laser beam passes through. These two monitoring beams experience lower, but approximately equal, transmission as compared to the laser beam. These lower transmissivities are identical if the laser is

oscillating at the value coincident with the transmission peak of the etalon; however, if this peak shifts, as due to the Moiré fringe mechanism discussed below, there will be an imbalance in the two signals to the feedback stabilization system.

The error signal is proportional to the shift of the supermode resonance from the transmission peak of the pulse repetition rate etalon. The relatively large shift in the laser spectrum for a fraction of a wavelength change in the optical path in the resonator can be understood in terms of a Moiré fringe condition. This condition is related to the detuning of the modulator frequency from the free spectral range of the pulse repetition rate etalon. The relationship of the laser modes that oscillate to the transmission peaks of the pulse repetition rate etalon is illustrated in Fig. 2.

In Fig. 2a, the central resonance in the figure is coincident with a given mode of the overall resonator. The detuning of the modulator frequency and the pulse repetition rate etalon free spectral range causes the modes of the overall resonator to be successively detuned by progressively larger amounts. There are also in the actual system many other supermodes that do not coincide with a transmission peak. The figure exaggerates the width of the transmission peaks for the purpose of the illustration. In practice, there are some 200 possible distinct supermodes that lie between each of the transmission peaks. These are suppressed in an optimal system and do not oscillate.

A small change in the overall resonator length by a fraction of the optical wavelength causes a displacement of the total resonator mode position. For example, the FWHM of the resonator peak is 8.66 MHz hence a shift of 1 MHz in mode position causes a significant shift of the mode relative to the resonator transmission peak. The mode separation is ~6 MHz. Thus a change in optical path by a fraction of a wavelength can cause a significant shift of the laser spectrum via a kind of Moiré fringe mechanism. This shift produces an error signal via the differential change in the signals transmitted to the two detectors that drive the feedback electronics. Such a shift can also lead to two supermodes symmetrically located under a single transmission peak of the etalon and hence since shifts must be controlled.

As a means of bringing the beam into the free space region and supporting the mirrors that introduce and remove the beams that pass through the wedged etalon, we use Newport Ultra-Align xy and xyz positioners. The collimating lenses were 8 mm focal length laser diode collimating lenses. In general, all optical surfaces

other than the fiber ends were anti-reflection coated. The fiber ends were cut at an angle of 8 degrees. The xy and xyz positioners have sufficient stability that we can adjust their alignment and then leave them at those positions from day to day without need for readjustment.

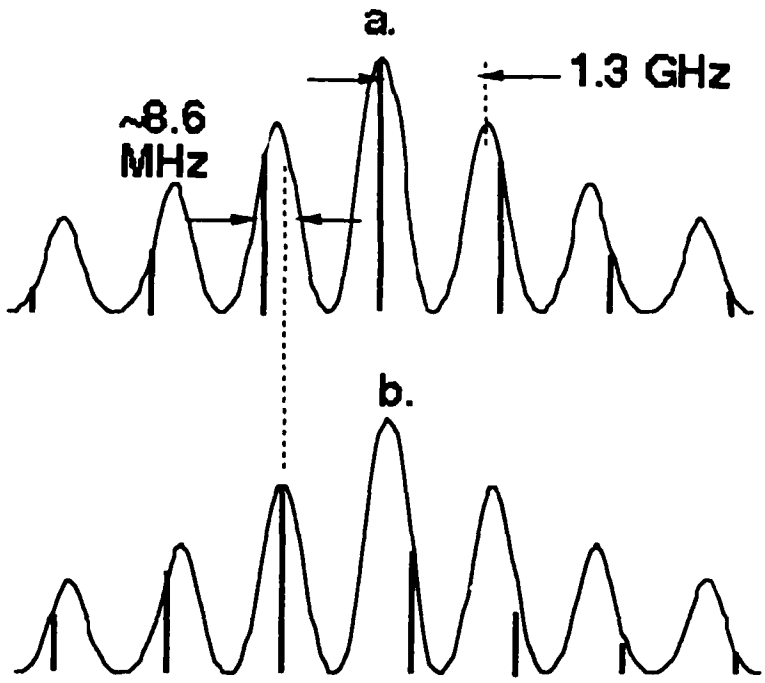

Fig. 2. Relationship of resonator modes to the transmission peaks of the pulse repetition rate etalon.

4. FIBER COMPONENTS

The fiber components consisted of two isolators, a length of erbium fiber excited by 980 nm pump light introduced by a WDM 1550/980 mixer, a polarization controller, an AT&T modulator capable of modulating the beam at rates up to 10 GHz, a piezo-electrically driven fiber stretcher, (or a section of lightly doped erbium fiber that had been coated with metal and could be length tuned by passing a current through the metal coating), and

an output coupler. The isolators were formed by Faraday rotators located between two polarizers. Two isolators were used to provide additional discrimination against back reflections. The erbium fiber was either a 20 meter long section or a 10 meter long metal coated section mentioned above. The modulator was capable of being operated in a balanced mode although it was typically used unbalanced. The pump power ranged from about 250 mW downwards. Threshold for lasing varied from 30 to 100 mW, depending on the components in the laser.

The output coupler was a 30/70 coupler with the 30% fraction exiting the laser. Other couplers were used to divide the laser beam among the various diagnostic devices. The polarization controller was a three paddle device made by BT&D. The coupling of the pump light to the fiber was performed using a Newport F-1015 high precision single mode fiber coupler. In general, we were able to couple about 50% of the pump light into the fiber. The coupling was stable from day to day; however, occasional readjustment was required, especially if the alignment of the pump laser was changed. All the couplers were from Gould. The light directed to the diagnostic equipment such as the Princeton Applied Research Optical Multichannel Analyzer (OMA) and the photodetector for the rf spectrum analyzer used free space collimation of the laser beam. For the OMA the beam illuminated the slit of a Jarrel-Ash 1/4 meter spectrometer. The coupling to the fast photodiode used for the high speed oscilloscope was done via a fiberized connection to the diode.

5. PUMP SOURCE AND DIAGNOSTIC EQUIPMENT

The pump was provided by a Ti:sapphire laser excited by an Innova-200 Coherent, Inc. argon laser operating multiline at about 13.5 Watts output. Pump powers at 980 nm from the Ti:sapphire laser were 200 to 500 mW and corresponded to powers of 100 to 250 mW delivered to the erbium fiber section. Special problems were the need to realign the Ti:sapphire laser, clean the mirrors and lenses frequently, and to adjust the emission wavelength so as to fall within the erbium absorption bandwidth. Alignment of the Ti:sapphire laser requires some means of monitoring the emission wavelength during readjustment. We constructed a small spectrometer consisting of a grating and a calibrated infrared card readout that allowed this monitoring, or else used the OMA.

A 1 GHz Hewlett-Packard signal generator was used as the signal source. The drive frequency was doubled by a Minicircuit electronic doubler to 1.36 GHz. Means for diagnosis were a scanning Fabry-Perot interferometer having a 100 GHz free spectral range, a 6 GHz bandwidth oscilloscope in combination with a 25 GHz

bandwidth NuFocus photodiode, and a PAR optical multichannel analyzer (OMA) with an InGaAs detector array. The OMA was used to observe the optical spectrum of the pump and the laser itself. A round trip ~ 2 km long optical fiber path, to the Science Center at RPI was included as an exercise in using an optical link as part of the system.

This combination of diagnostic equipment is important in constructing, operating, and studying this laser. The different diagnostic devices provide cross checks on each other and allow a more accurate determination of the state of the laser. For example, the rf spectrum analyzer not only shows the fundamental beat frequency, but also provides a measure of the onset of additional supermodes. The beat frequency between the supermodes creates an additional weak component in the rf spectrum shifted from the primary peak by the mode spacing frequency of the overall resonator. In some cases, higher order beats can be seen. These provide a measure of the onset of the additional unwanted supermodes. The scanning Fabry-Perot provides a description of the individual components of a given supermode with the relative intensities and absolute positions of the modes clearly exhibited. In general, the regular envelope of the Fabry-Perot spectrum is lost when additional supermodes are excited providing an additional means of detecting that condition.

The display on the Tektronix oscilloscope is also informative of more subtle properties of the laser action. The envelope of the pulse as displayed on the oscilloscope reveals the presence of instabilities in the form of variations in the pulse envelope. When the pulse repetition rate etalon is introduced and the laser caused to oscillate in a mode pattern, such as illustrated in Fig. 3, the envelope of the pulses on the oscilloscope becomes very regular and smooth. If a single supermode is not selected, then the pulse envelope shows significant irregularities that change relatively rapidly in time.

6. SPECTRAL CONSTRAINTS ON THE HARMONICALLY MODELOCKED LASER

Three different constraints on the spectrum are included in the laser. These were the spectral filter, the wedged etalon, and the pulse repetition rate etalon. The spectral filter, a narrow band interference filter, could be tuned by rotating the filter. This provided an ~ 2 nm (270 GHz) wide tunable pass band that controlled the spectral region over which the laser oscillated. The wedged etalon further limited the spectral range. The adjustment is accomplished by varying the position on the wedge where the laser beam intersects the filter. The pulse repetition

rate etalon further restricted the pulse spectrum. The etalon has a free spectral range was 1.36 GHz and a finesse of about 150.

In effect the presence of the pulse repetition rate etalon selects out a single supermode provided the transmission peaks are sufficiently narrow to allow only one resonator mode to oscillate at a given time and the relationship of the overall pathlength, the center of the wedged etalon transmission and the pulse repetition rate etalon spacing are such as to locate one of the allowed modes of the overall resonator near the center of a transmission peak of the pulse repetition rate etalon.

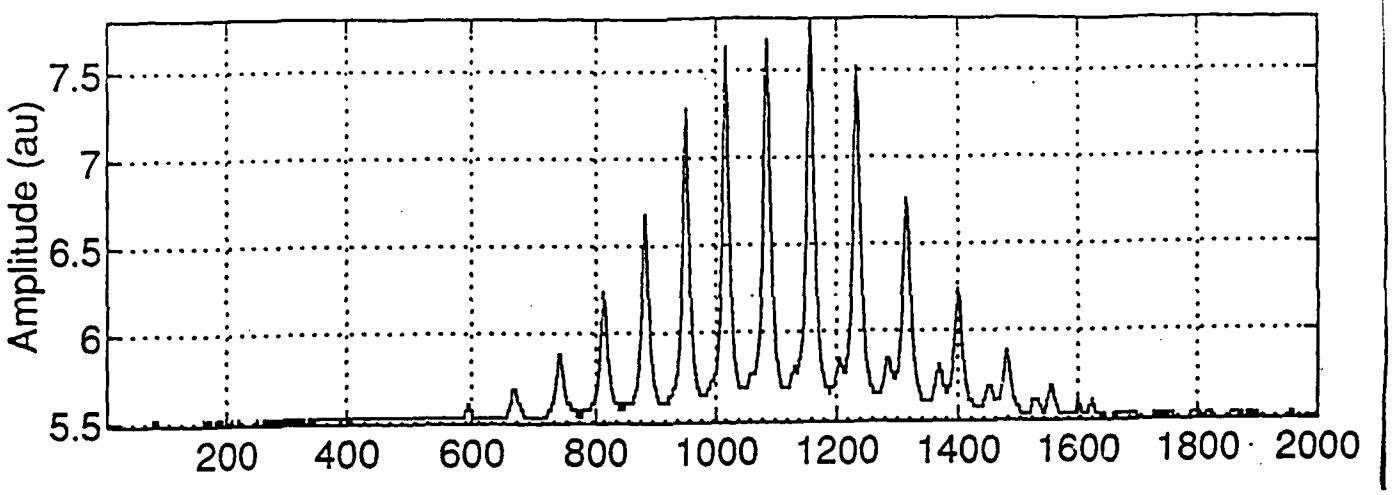

Fig. 3 shows a plot of the spectrum of the output of the laser. The mode spacing was 1.36 GHz and the FWHM of this spectrum is 8.7 GHz.

In general, where we measured the pulse duration and spectrum, the pulses were near transform limit. This spectrum consequently implies a pulse width of about 50 ps. The oscilloscope display in this case was limited by the bandwidth of the oscilloscope, but was consistent with this duration.

In the initial realization of the laser about 10 modes oscillated at a given time producing pulses of about 45 ps duration. (The full width at half maximum of the spectrum is about 6.6 GHz, which is consistent with approximately transform limited pulses). Larger bandwidths are, of course, required for shorter pulses. Efforts are being made in this direction. In general, the primary constraint on bandwidth is the detuning; of the pulse repetition rate etalon and the modulator. This detuning is needed to provide the error signal, but creates an effective bandwidth limiting process. Larger bandwidth can be gained by causing the pulse repetition rate etalon free spectral range to approach the modulator frequency, but this reduces the error signal. (see Fig. 2). Some compromise must be found between the need for detuning to produce the error correction signal and the desire for a large bandwidth.

7. PULSE REPETITION RATE ETALON

We provide here additional information on key components. The pulse repetition rate etalon needs to be well aligned with the other components and excited by means of a well mode matched beam. A computer program was written for identifying the mode matching conditions given the leans focal length and the radii of curvature of the mirrors. In the absence of the pulse repetition rate etalon, the pulse envelopes are irregular and fluctuate in time. The pulse to pulse stability is also irregular.

The pulse repetition rate etalon free spectral range must be an integral multiple of the mode spacing of the overall laser, or stated in other terms, the laser path must be an integer times the mirror spacing of the repetition rate etalon. In practice this requires some means of adjusting the overall pathlength in the resonator so that this condition is satisfied. We found in practice this can be done either by trimming fiber, or more easily, by incorporating a free space adjustable delay line. While small detunings are possible and some degree of adjustment can also be achieved by varying the wavelength of the laser, it is in general desirable to include some means of adjusting the overall pathlength of the laser. Also the need for the mirror spacing of the repetition rate etalon to be highly stable and for the laser beam to be mode matched into that resonator places practical constraints on the design of the structure that holds the mirrors in position.

We constructed the initial etalon out of conventional good quality mirror mounts, e.g., Klinger SL series mounts with differential screw adjusts. We found that the stability of these

structures was questionable and replaced that structure with a super-invar etalon sold by Burleigh. This structure proved adequate, but has the constraint that the mirrors are epoxied into position and consequently do not offer the conventional means of independent mirror adjustment. Alignment can be achieved by a strategy where the mirrors are permanently epoxied in position so that they are close to correct alignment and then achieving final alignment by orienting the entire etalon structure within the laser path so as to selectively excite the lowest order mode of the resonator. In practice we found it useful to use both .633 micron He-Ne laser emission and also 1.52 micron He-Ne laser emission for the alignment. The .633 micron light probes the full resonator even if the mirrors are far enough off alignment that the lowest order mode is not efficiently excited. The 1.52 micron light is needed to view the transmission spectrum and determine the degree to which the alignment excites selectively the lowest order transverse mode.

The equations for mode matching can be found in reference 5. It is important to use these equations in determining the proper lens and component spacing in matching the incident light into the interferometer. It is also important to have some means of monitoring the transmission spectrum of the interferometer during the alignment. In practice we accomplished this by including a piezoelectric scanning element in the interferometer and driving it with a Burleigh RC-44 ramp generator.

8. FEEDBACK SYSTEM

We provide here additional detail concerning the feedback system. The wedged etalon and the means of introducing and extracting the monitor beam are described above. The two photodetectors (EG&G Judson InGaAs) provide the input to the feedback circuit. The electrical power out is about 150 mW each. The nature of the differential feedback signal can be understood by reference to the spectrum of the laser. The relationship of the laser emission spectrum to the transmission peaks of the pulse repetition rate etalon is shown in Fig. 2. An actual laser spectrum is shown in Fig. 3. The regular nature of the spectrum is evident.

When the pulse repetition rate etalon is included in the resonator the laser spectrum remains stable in shape. The absolute positions of the individual modes that oscillate are determined by the optical path of the overall resonator. These individual oscillating modes shift slightly as the optical pathlength of the ring changes slightly due to thermal drifts, e.g.. These small shifts can cause large shifts in the envelope of the laser

spectrum shifts. These shifts of the envelope tend to be large compared to the free spectral range of the pulse repetition rate etalon. These shifts can be less than, or more than the spectral bandwidth depending on the degree of detuning of the modulation frequency and pulse repetition rate etalon free spectral range. This envelope shift for a small change in optical path is the "Moiré fringe" mechanism described in the original paper on harmonic modelocking including a Fabry-Perot stabilizing element.[1] Too small a detuning fails to produce a sufficiently sensitive error signal to the feedback loop. Too large a detuning unnecessarily limits the bandwidth of the laser.

In the experimental laser, the laser spectrum remains stable in position for a period of time sufficiently long to take the interferometer trace, but otherwise tends to drift on the time scale of a few seconds. The means of correcting these variations in fiber length that are being explored are: a metal coated fiber that can be varied in length by varying the heating current to the metal coating; a piezoelectrically stretched fiber.

The metal coated fiber was loaned by AT&T. The piezoelectrically stretched fiber is a commercial unit sold by Canadian Instrumentation. The amount of correction of the pathlength that can be achieved is about 10^{-5} of the fiber length wound on the stretcher. The coefficient of thermal expansion for fused silica is 0.5x10-6 deg C. Thus for a 20 degree temperature variation, the thermally induced change in the length of the fiber path is comparable to the maximum change produced by the stretcher. It is thus important to keep the total fiber path at a minimum and the length of fiber on the stretcher a large fraction of the total length. In practice, these considerations require that the 10-20 meters of fiber used for the erbium amplifier be wound on the stretcher, and that other fiber lengths in the laser be minimized.

One of the particular difficulties that must be recognized in using the piezoelectric stretcher is that additional bending losses are encountered in the fiber when it is wound on the fiber stretcher. We found that a one inch radius on the mandrel that supported the fiber was insufficient as regards the need to avoid unacceptable bending losses in the fiber. We found, e.g., 4.5 dB loss for 10 meters of fiber wound on a one inch diameter mandrel. The decision has been to use a diameter of two inches or larger for the mandrel. Another concern is that the installation of the fiber on the mandrel be performed in a manner that maintains firm contact of the fiber with the mandrel, but otherwise allows removal of the fiber. This allows varying the length of erbium

doped fiber without requiring replacement of the fiber which tends to be expensive.

We have investigated the length of erbium doped fiber that is needed in the laser. Three lengths of erbium doped fiber were available. One length was 20 meters of lightly doped fiber. The second length was 10 meters of lightly doped fiber. The third length was about 2 meters of heavily doped fiber. The most favorable case was the 20 meter length of lightly doped fiber. This provided the largest gain. The 10 meter length was adequate to cause laser action and pulse formation. The heavily doped short section of fiber was not adequate to provide the necessary gain in the laser.

The effective optical pathlength in the laser that we find is acceptable is about 50 meters. This gives a mode spacing of 6 MHz. The actual physical path is consequently about 30 meters, given that the bulk of the path is in fiber and the refractive index of the fiber is 1.46. This path is sufficient to accommodate the 20 meter length of the erbium doped fiber and the additional free space components, but not so long as to introduce instabilities caused by two supermodes modes falling within the pass band of the pulse repetition rate etalon.

We explored the consequence of introducing an NOLM loop. In the NOLM loop a differential nonlinear phase shift provides nonlinear optical pulse shaping in the laser. The observation of additional supermodes on introducing the longer length required by the NOLM suggests considering alternative means of nonlinear pulse shaping.

We also explored the operation of the laser for the case of strong pumping where we adjusted the polarization controller and looked for evidence of pulse shortening by soliton formation or pulse shaping caused by nonlinear polarization rotation. In general, we did find that for sufficiently energetic pulses, the adjustment of the polarization controller could lead to a broadening of the emission spectrum consistent with the reduction of the pulse duration to a few picoseconds. The operation of the laser under these conditions was irregular and would not be adequate for the stable ultrashort pulse conditions sought.

The implication however, is that if we include nonlinear shaping via polarization rotation or some other means that does not introduce additional supermodes, there is an opportunity to achieve high repetition rate, ultrashort pulses, and stability in a single laser.

9. EXPERIMENTAL FIGURE EIGHT VERSIONS OF THE LASER

On introducing the NOLM loop in the experimental laser, we found the rf spectrum revealed multiple supermodes oscillating simultaneously. We also observed the envelope of the pulses became less regular. The onset of this mechanism suggests physical pathlengths (note that optical pathlengths are about 1.46 times the physical pathlength) longer than 30 meters are undesirable. On the other hand, the nonlinear loop mirror needs to be relatively long (see ref 4) if sufficient nonlinear shaping is to be obtained to reduce the pulse duration. The problem is that too short a loop length does not produce a large enough nonlinear phase shift to gate the loop open. This implies the NOLM is not the best strategy.

We briefly explored obtaining the nonlinear shaping in a NALM loop. The NALM includes the erbium fiber and in principle allows a shorter laser pathlength. A NALM loop was introduced but did not show evidence of stable pulse shortening. The trial was not pursued in detail. One of the weaknesses of this approach is the variability of the polarizing properties of the fiber path. We did include in the loop a polarization controller to allow control of the polarization. This control also provides, in effect, control of the coupling ratio in the NALM, since this ratio depends on the polarizing properties of the loop.

The goal of a highly stable laser suggests alternatives to the NALM and NOLM loops be pursued. We discuss below numerical simulations we used as a guide in exploring the laser and the influence of the nonlinear loop in general.

10. NUMERICAL SIMULATIONS OF THE HML LASER

In this section we describe numerical simulations used to explore performance of the laser. These simulations provide information concerning pulse shortening and the need for nonlinear pulse shaping.[4] While the work under this project suggests the NOLM loop will probably not be the preferred means for nonlinear shaping, the results do show the importance of including nonlinear shaping and clarify preferred strategies.

The parameters used in simulating the laser performance are those of the experimental laser under construction. This simulation includes essentially all the properties of the laser with the exception of the pulse repetition rate etalon. To include the etalon would require simulating the entire pulse train. That computational task requires an amount of computer time that would be prohibitive on currently available computers. The program and

the accompanying documentation has been written in the form of a doctoral dissertation by one of the students in the Ultrafast Photonics Group, Kalwant Singh.[4] The dissertation is on file at the RPI library in Troy, New York.

The simulations also describe the laser dynamics. These calculations provide a measure of the time it takes for the laser to respond to a change in the operating conditions. This includes both the start up of the laser and the response of the laser to an external control signal introduced in the nonlinear element. The stabilization generally occurs within less than 10 round trips around the laser path. The resolution of the timing in the simulation is a small fraction of the pulse duration.

A simple strategy for shortening the pulse is introduction of a comb generator. The comb generator shortens the duration of the pulse driving the modulator. The modulator cannot now produce gate widths much less than about 100 psec; however, we show in Fig. 4, for purposes of evaluating the potential of shorter gating times, the dependence of the pulse duration in the laser on gating widths ranging down to a picosecond. The shorter modulator gate durations in this plot are not now and may never be accessible by electronic means in practical systems. Some optical means of gating the pulses thus appears essential.

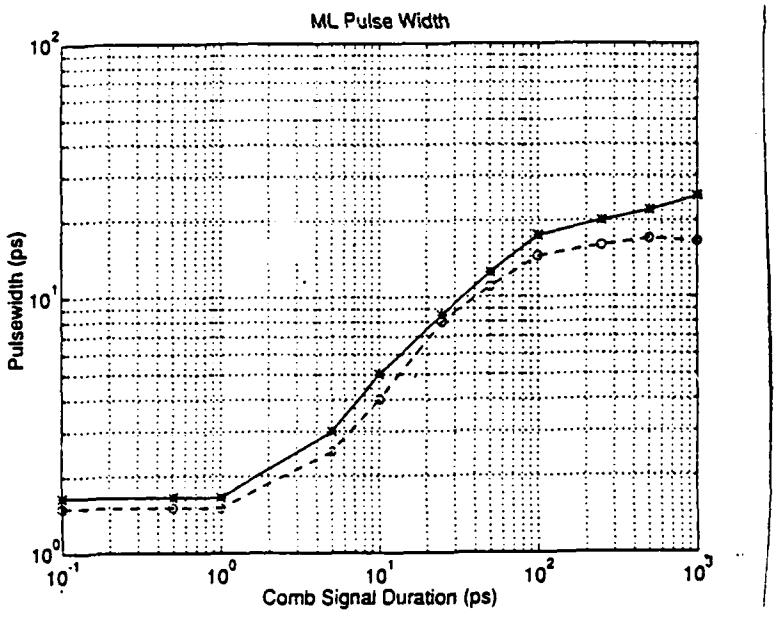

Fig. 4 Numerical simulation of pulse duration vs. gate width.

Given the need to introduce nonlinear pulse shortening there remains the task of identifying the best strategy. We explore here specifically the NOLM structure. The numerical simulations explored the laser performance under a variety of conditions. The principal finding was that the nonlinear optical shaping can be used to reduce the pulse duration to values less than one picosecond for operating conditions that are representative of the experimental laser. The experimental work, however, revealed that the added length of the NOLM loop resulted in the simultaneous oscillation of more than one supermode in a manner that compromised the stability of the laser. The conclusion is that more highly nonlinear loops are preferred that allow shorter paths, or else some alternative means of nonlinear shaping.

Returning to a description of the simulation work, the bandwidth was modeled by defining a spectrally limiting element and modeling the performance of the laser under that constraint. In practice, there are several sources of bandwidth constraint that can be varied. These are the spectral filter, the wedged etalon, and the detuning of the modulator frequency and the free spectral range of the pulse repetition rate etalon. We have assumed a limiting bandwidth for the laser of 0.5 nm, or 62.5 GHz, comparable to the wedged etalon full width at half maximum.

11. NUMERICAL SIMULATION OF THE LASER INCLUDING A NOLM LOOP

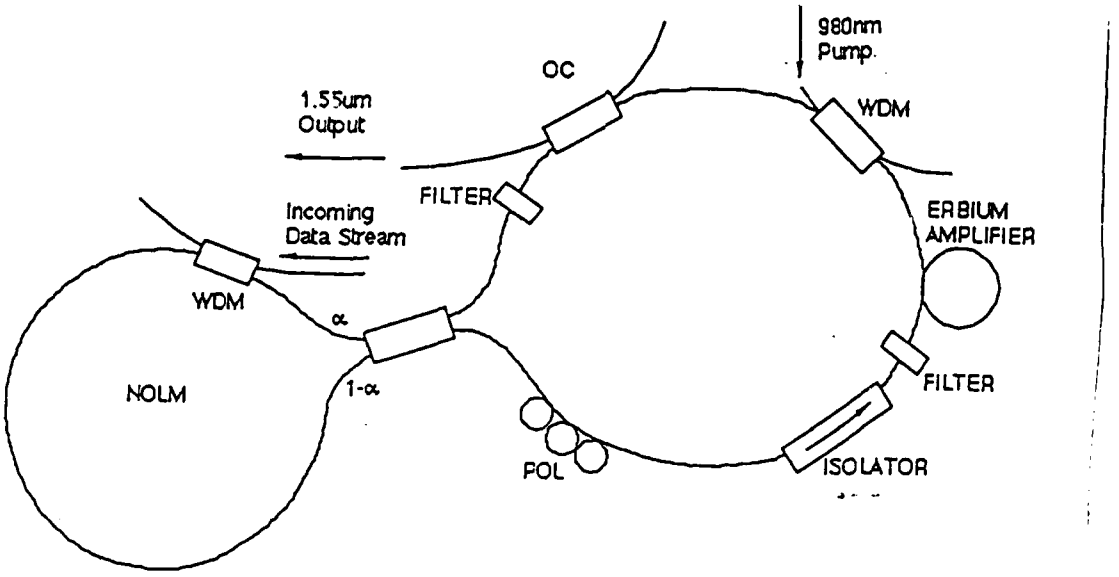

Fig. 5. HML laser including the NOLM loop and key components.

The structure of the laser on adding a NOLM loop to the experimental HML configuration is illustrated in Fig. 5. As expected, the numerical simulation indicates the NOLM loop can significantly shorten the pulse duration. The simulations indicate the pulse durations are eventually limited by dispersive wave radiation as observed in previous work on figure 8 lasers.[6,7]

In the simulation model, the NOLM is located immediately after the output coupler so as to maximize the pulse energy introduced into the NOLM, while still maximizing output power. An adjustable coupler divides the power coupled into the two arms of the NOLM by amounts α and $1-\alpha$. Simulations were carried out for NOLM split ratios of α = 0.2, 0.3,0.4,0.45 for NOLM loop lengths ranging from a few tens of meters to several hundred meters. Pump powers were fixed at 200 mW, internal losses (excluding NOLM losses) were 6 dB, while the output coupling was 30%.

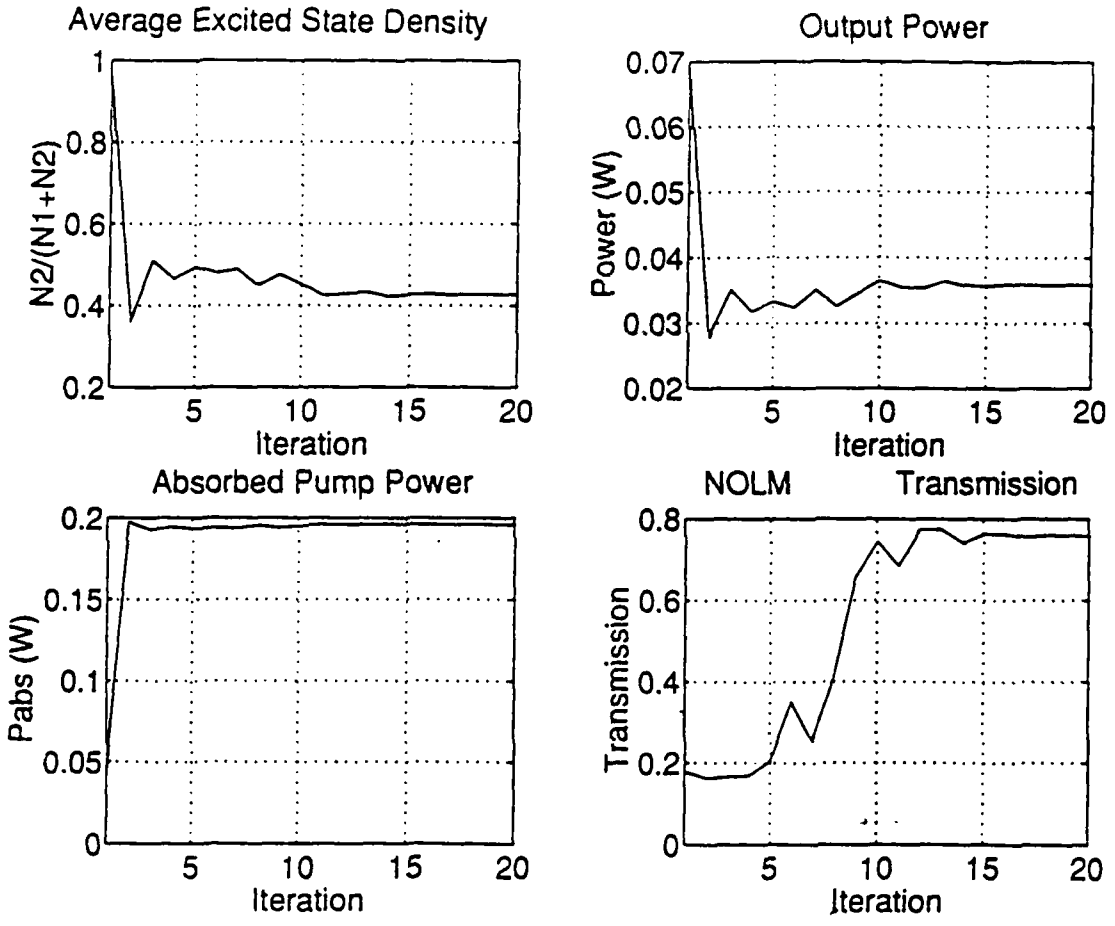

Fig.6 Sample diagnostics for the fiber laser including a NOLM loop

The erbium fiber length was 20 m for α = 0.2, 0.3, but was increased to 30 m for a = 0.4, 0.45. This ensures the unsaturated small signal gain exceed the total system loss given by the sum of the internal losses, output coupling losses and low field transmission given by $(1-2\alpha)^2$.

Initial conditions for sustained lasing were thus met. The spectral filter bandwidth was set at 0.5 nm (FWHM) centered at 1.553 microns. The modulator in this simulation was modeled as driven by a sinusoidal signal, as there was no change in the pulsewidth when a shorter pulse, as produced by a comb signal, was substituted. This implies the NOLM is the primary shortening mechanism.

Diagnostic outputs of a typical computational run (α=0.3, L_{nolm} =50 m) can be provided as an illustration of the predictions of the software. An initial measure of stability of the computer run can be made by monitoring the convergence rate of the laser parameters shown in Fig.6.

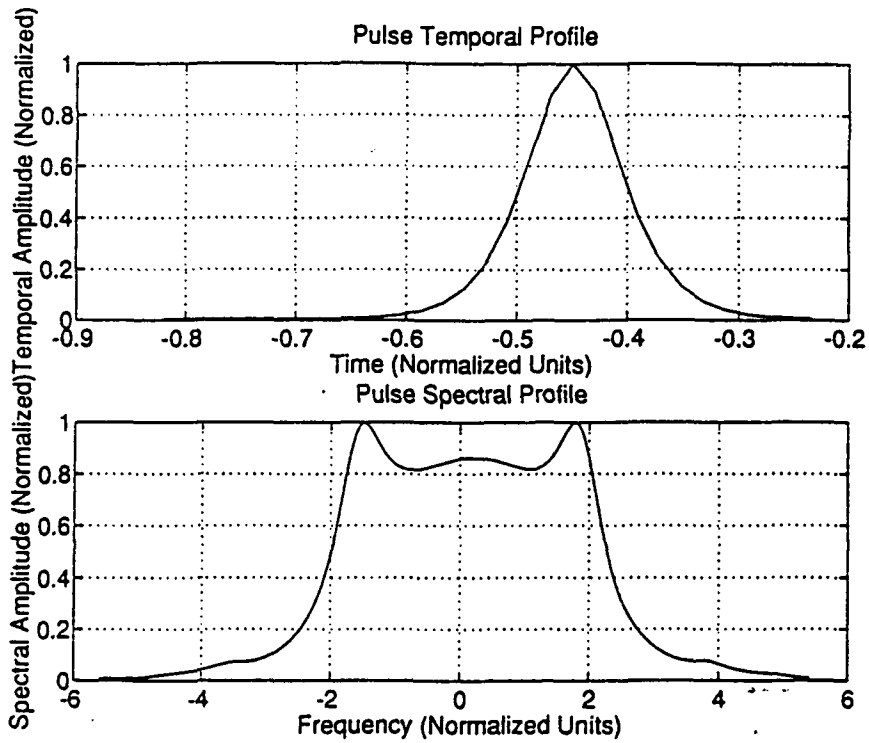

Fig. 7 Sample pulse duration and spectrum for the fiber laser including the NOLM loop. The assumed bandwidth imposed by the spectrally limiting elements is 0.5 nm.

The state of the NOLM transmission as a function of the iterative cycle provides a measure of the effectiveness of the NOLM. Fig. 6 indicates that the NOLM transmission increases from the initial low field value of $(1-2\alpha)^2 = 0.16$ to a value approaching 0.8 after 20 iterations. The NOLM transmission does not reach 100% (as expected for an ideal soliton) due to pulse shape distortion that results from dispersive wave radiation losses. The erbium fiber is heavily saturated when convergence is reached as can be seen from the low value of average excited state density (0.43).

Fig. 7 illustrates the pulse temporal and spectral profile at the end of 20 iterations. Each normalized unit in the figure is equivalent to 5 ps. Each normalized frequency unit is equivalent to 1/5 ps or 200 GHz. The FWHM pulsewidth is about 500 fs, while the FWHM spectral width is about 0.76 THz. The time-bandwidth product is ~ 0.38.

The relationship between pulsewidth and the total NOLM laser loop length is shown in Fig. 8 on a log-scale for $\alpha = 0.3, 0.45$. A linear best fit to the computational points is also shown. The slope of the line is 0.5, with the relationship between the pulsewidth ($t_{(FWHM)}$ in seconds) and total loop length (L in cm) given approximately by

$$t_{(FWHM)} = 5.7 \times 10^{-15} \, (L)^{1/2} \qquad (1)$$

In general, dispersive wave radiation restricts the minimum pulsewidth achievable in fiber loop lasers according to the relation $t_{(FWHM)} \sim (\beta_2 \, L)^{1/2}$. The value obtained for the dispersion parameter β_2 from data for standard fiber is 10^{-28} s^2/cm which yields (1) above.

The good agreement between the relation found above in the numerical simulation and the theoretically predicted dispersive wave limited pulsewidth is consistent with the expectation that the pulsewidth is limited in this model by dispersive wave radiation. A similar fit has been reported as experimental evidence for dispersive wave radiation as the limiting mechanism in passively modelocked NOLM erbium fiber lasers.[8]

Dispersive wave radiation thus is expected to limit the minimum pulsewidth to about 500 fs in the absence of strategies to reduce its importance. The simulations shown above were repeated

including the effects of stimulated Raman scattering, self steepening, and third order dispersion. No differences were observed.

In this model, there is a limit to the degree to which the NOLM loop length can be reduced to obtain short pulses. Loop lengths shorter than those used to obtain the above simulations resulted in unstable oscillations. These unstable oscillations can be attributed to a nonlinear phase shift too small to give adequate transmission through the NOLM. Similar limitations were observed experimentally in passively modelocked NOLM fiber lasers[2,3].

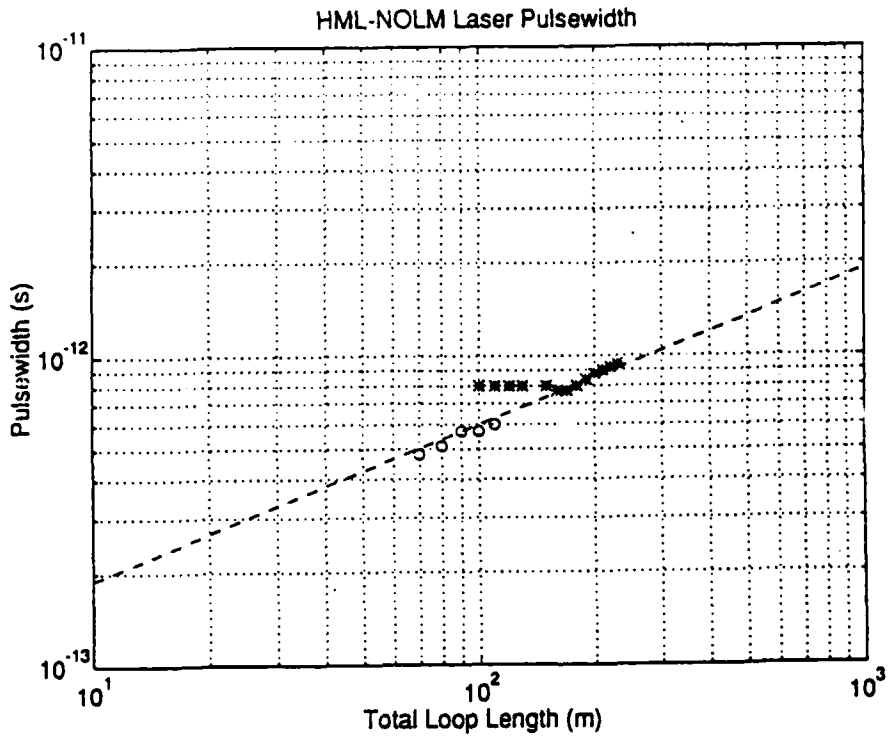

Fig.8 Pulsewidth versus total loop length for fiber laser including an NOLM loop on a log-log scale. The assumed spectral bandwidth is 0.5 nm. The cases treated are for α=0.3 (open circles) and for α=0.45 (asterisks).Dashed line is a linear best fit.

We conclude that it would be helpful to introduce a fast saturable absorber with a fast recovery that functions in the manner of the NOLM, but that introduces as little additional pathlength as possible. The NALM is preferable to the NOLM in this regard in that it produces similar nonlinear shaping, but permits a shorter laser since the erbium doped fiber can be included as part of the nonlinear path. Other attractive alternatives would be the incorporation of a polarization based switch that required less additional length or a spatial soliton switch[8].

12. SYNCHRONIZATION OF HML LASERS THAT INCLUDE NONLINEAR GATES

The introduction of a nonlinear optical pulse shaping element not only provides means for generation of shorter pulses, but also creates an opportunity for synchronization of two or more of these lasers via the action of an externally introduced pulse acting on the nonlinear element.

Nonlinear optical mechanisms have been used for clock recovery.[9] The laser shown in Fig.4 includes a modification of the NOLM structure that provides means for synchronizing the laser with an externally introduced pulse train.(The control pulse in this example is prevented from propagating through the harmonically modelocked laser loop by spectral filters.) The control pulse influences the initiation of pulsing in the HML laser including a NOLM. The temporal development of the transmission of the NOLM loop is illustrated in Fig.9 for the case where there is no external control signal (dashed line) and for the case where there is a control signal (solid line).

The control pulse spectrum has been chosen to be slightly different from the controlled pulse spectrum so that the control pulse walks across the controlled pulse temporal width during the transit within the NOLM loop. The decreased transmission of the loop at later times in the presence of the control pulse we attribute to a small, cross phase modulation induced distortion of the controlled pulse by the externally introduced control pulse. This distortion can be seen in simulation plots of the signal pulse envelope (not shown here).

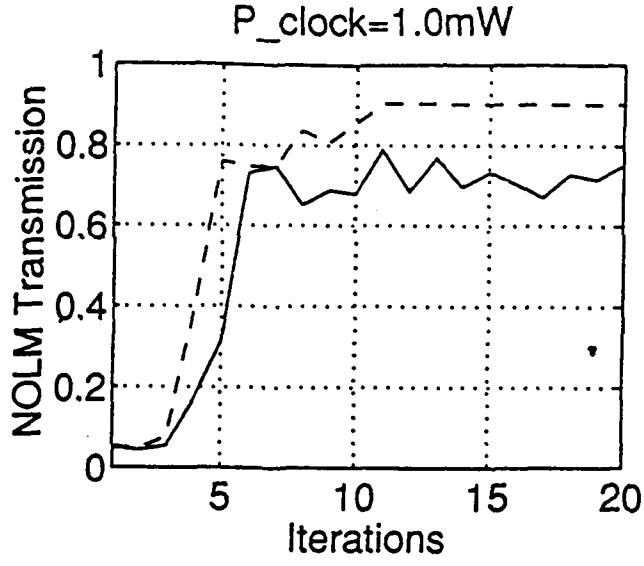

Fig. 9. Transmission of NOLM loop for the case of no control pulse (dashed) and for the case of a control pulse present (solid).

The evolution in time of the controlled pulse from its original temporal position (assumed to be initially shifted from the relative mean position of the control pulse) to a temporal position determined by the control pulse is illustrated in Fig.10. Convergence to the final temporal position occurs within about 50 round trip transits. It appears desirable to choose a level of control pulse intensity that is not too low, in which case control is not effective, or too high, in which case the controlled pulse can be distorted by cross phase modulation. The acceptable range of values is not broad, but appears sufficiently wide to be useful.

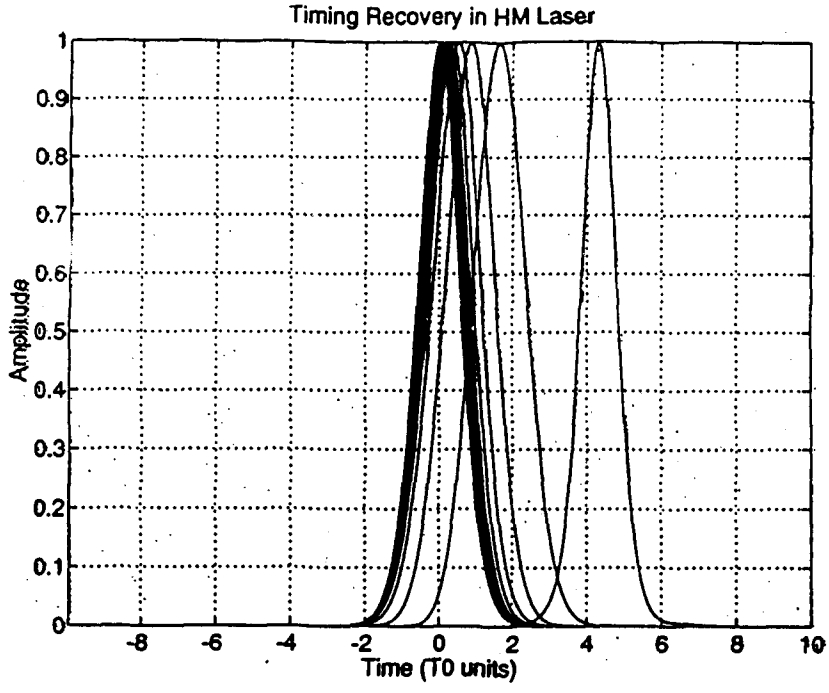

Fig. 10 Evolution in time of the controlled pulse in the gated fiber laser as caused by the externally introduced control pulse.

13. SOLUTIONS

The important next step appears to be retaining the stabilizing features of the current laser while adding nonlinear optical pulse shortening in a form compatible with the stabilizing features. One recent advance that appears useful is the development of a single polarization fiber amplifier combined with an environmentally stable strategy for modelocking. The single polarization amplifier is described by Duling.[6] A related strategy is described by Fermann.[7]

These strategies use a section of fiber that is not polarization constraining, a Faraday mirror, a section of the laser that does constrain the polarization, and a region where a bias can be introduced so as to favor some nonlinear rotation of the polarization state of the laser.

The switching is accomplished by the nonlinear rotation of the polarization state in the birefringent fiber. This is accomplished in the work of Fermann for the case of pulses of 60 pJ energy. For the higher pump rates made possible by recent advances in diode pump sources it should be possible to use these approaches at higher rates allowing the contemplated gigabit repetition rates in combination with stable operation.

14. CONCLUSIONS

The conclusion of this work is that the strategy of using modelocked fiber lasers operating at 1.55 microns as a source of stable pulse trains of ultrashort optical pulses a gigahertz repetition rates is sound. It does appear desirable to explore means of introducing nonlinear optical pulse shortening that retain fiber pathlengths of the order of 30 meters or less. In practice, it appears that a polarization rotation switch used in combination with the stabilizing features already included in the current laser is a desirable direction.

15. ACKNOWLEDGMENTS

We express appreciation for valuable help from George Harvey and Linn Mollenauer of AT&T Bell Laboratories and Steve Johns and Reinhard Erdmann of Rome Laboratories. In addition to Rome Laboratory, some of the work performed here used equipment provided by AFOSR, ARO, NSF, and RPI grants.

16. REFERENCES

1. G.T. Harvey and L.F. Mollenauer, "Harmonically modelocked fiber ring laser with an internal Fabry-Perot stabilizer for soliton transmission", Optics Letters 18, pp. 107-9, January 1993.

2. I.N. Duling III, "Subpicosecond all-fiber erbium laser", Electron. Lett., 27, 544 (1991).

3. Song Wu, Jefferson Strait, Richard L. Fork, and T.F. Morse, "High-power passively mode-locked Er-doped fiber laser with a nonlinear optical loop mirror", Optics Letters 18, 1444-6 (September 1, 1993).

4. K. Singh, "Simulation and analysis of erbium fiber lasers and amplifiers with application to the harmonic modelocked non-linear optical loop mirror laser", PhD Thesis, Rensselaer Polytechnic Institute, Troy, NY (November 1993).

5. R.L. Fork, D.R. Herriott, and H. Kogelnik, "A scanning spherical mirror interferometer for spectral analysis of laser radiation," Applied Optics Vol. 3, No. 12, 1471-1484 (December 1964).

6. I.N. Duling III and R.D. Esman, "Single polarization Fiber Amplifier", Electron. Lett, 28, 1126 (1992).

7. M.E. Fermann, L., L.-M. Yang, M.L. Stock, and M.J. Andrejco, "Environmentally Stable Kerr-Type Mode-Locked erbium Laser Producing 360 fs pulses," Optics Letters 19, 43 (1994).

8. A. Villeneuve, J. S. Aitchison, J.U. Kang, P.G. Wigley, and G.I. Stegeman, "Integrated Ultrafast Saturable Absorber". to be published in Optics Letters

9. A.D. Ellis, K. Smith and D.M. Patrick, "All optical clock recovery at bit rates up to 40 Gbit/s", Electronics Letters, Vol. 29, No. 15 1323-4 (July 22, 1993).

*U.S. GOVERNMENT PRINTING OFFICE: 1994-510-117-50017

MISSION

OF

ROME LABORATORY

Mission. The mission of Rome Laboratory is to advance the science and technologies of command, control, communications and intelligence and to transition them into systems to meet customer needs. To achieve this, Rome Lab:

a. Conducts vigorous research, development and test programs in all applicable technologies;

b. Transitions technology to current and future systems to improve operational capability, readiness, and supportability;

c. Provides a full range of technical support to Air Force Materiel Command product centers and other Air Force organizations;

d. Promotes transfer of technology to the private sector;

e. Maintains leading edge technological expertise in the areas of surveillance, communications, command and control, intelligence, reliability science, electro-magnetic technology, photonics, signal processing, and computational science.

The thrust areas of technical competence include: Surveillance, Communications, Command and Control, Intelligence, Signal Processing, Computer Science and Technology, Electromagnetic Technology, Photonics and Reliability Sciences.